Int. J. Solids Structures, 1975, Vol. 11, pp. 187–198. Pergamon Press. Printed in Gt. Britain.

STABILITY OF MASONRY PIERS

R. FRISCH-FAY

University of New South Wales, Kensington, N.S.W., Australia

(*Received* 11 *February* 1974; *revised* 18 *July* 1974)

Abstract—An analytical and a matrix displacement approach is utilized to obtain a load-deflection relationship of columns made of a material which can resist little or no tension. The theoretical investigation covers piers subject to eccentric loads. A rigorous solution is presented along with an approximate finite element method involving an incremental, step by step approach.

NOTATION

b width of pier
d depth of pier
e eccentricity at top of pier
A $2P/9Eb$
L length of column
EI bending rigidity
F, P axial load
H function of z defined in equation (10a)
$\mathbf{P}$ generalized load vector
k_E, k_G, K_E, K_G elastic and geometric stiffness
l length of column element
m, p moment and force on column element
s length of rigid connectors
t^2 $(\frac{1}{2}d - \delta)^{-1}$
$\mathbf{u}$ displacement vector
x, v coordinates
z distance of line of action of load from concave face
α reduction factor of I
β $1 + \sigma_t/\sigma_{av}$
β_1 $\frac{1}{2}(3 - \beta)$
γ $\frac{1}{2} - \delta/d$
δ eccentricity at bottom of pier
θ, u rotation and displacement of column element
Δ incremental operator
$\sigma, \sigma_t, \sigma_{av}$ compressive stress, tensile resistance, P/bd
μ Fl^2/EI
ν $\delta/d - \frac{1}{6}$

1. INTRODUCTION

The analytical investigation hinges on the fact that after cracking occurs the effective depth, d, of the section decreases while the cracked length of the column increases with increasing deflections. Because of this the column may be looked at as a bar with varying moment of inertia with the significant proviso that the variation of the inertia is unknown, and that it is not symmetrically placed about the material axis. If the column has zero tensile resistance cracking will occur at the slightest tendency for tension; stress distributions are trapezoidal in the uncracked zone and triangular in the cracked portion (Fig. 1).

If the column has a small amount of tensile strength such tension will build up on the convex

face at some sections in the uncracked zone, but once the tensile limit has been exceeded and the crack penetrates the cross section it is assumed throughout this discussion that stress concentration will preclude all forms but the triangular stress distribution (Fig. 1).

The problem of columns made of a no-tension material has been investigated by Angervo[1], Chapman and Slatford[2], Yokel[3], and Risager[4]. Columns, which in addition to axial loads have to carry lateral loads, have been considered by Hellers[5], and Sahlin[6]. Sahlin and Hellers[7] have extended the investigation to portal frames.

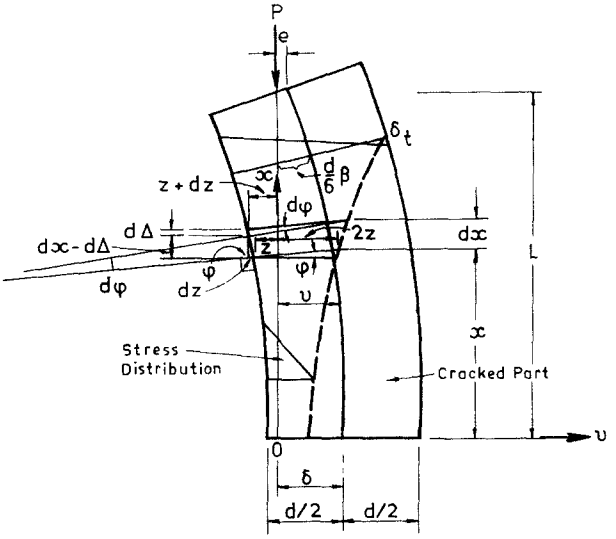

Fig. 1. Deflected shape of pier.

The versatile nature of finite elements suggests a displacement procedure for the load–deflection characteristics of columns whose effective depth is a function of the load and the deflected shape. Such a finite element procedure is feasible provided a member stiffness matrix is available that will cater for the changing geometry of the elements. Gallagher and Padlog[8] have shown that by taking derivatives of the "effective" strain energy the work done by the midplane loads is accounted for and leads to a force–displacement relationship which involves a stiffness matrix in addition to the conventional one. We may think of this additional matrix as the "incremental" or "geometric" stiffness. This method was successfully applied by Yang[9] for large deflection problems.

2. DERIVATION OF LOAD DEFLECTION EQUATIONS

The column to be analysed is of a rectangular cross section shown in Fig. 1. It is made of a material that can resist a small amount of tension $\sigma_t > 0$; the concentrated load P is eccentrically placed along the axis of the minor stiffness of the end section and $0 < e < d/2$.

In the cracked zone the stress at the compressed edge is

$$\sigma_x = \frac{2}{3}\frac{P}{bz} \tag{1a}$$

and the shortening at this edge of an element dx long is, from Fig. 1,

$$d\Delta = \sigma_x \frac{dx}{E} = 3z\,d\varphi. \tag{1b}$$

At the same time the slope φ (Fig. 1) equals

$$\varphi = \frac{dz}{dx - d\Delta} = \frac{dz/dx}{1-(2P/3bzE)} \tag{2a}$$

while its derivative, from equations (1a) and (1b)

$$d\varphi/dx = \frac{2P}{9bz^2E}. \tag{2b}$$

Differentiating equation (2a) with respect to x and equating it with equation (2b) results in

$$\frac{d^2z}{dx^2} - \frac{\frac{2P}{3bz^2E}}{1-\frac{2P}{3bzE}}\left(\frac{dz}{dx}\right)^2 - \frac{2P}{9bz^2E}\left(1-\frac{2P}{3bzE}\right) = 0. \tag{3}$$

Remembering that $(dz/dx)^2 \approx 0$ and $2P/3bzE \ll 1$, and introducing $v = \frac{1}{2}d - z$, the differential equation governing the cracked zone is

$$\frac{d^2v}{dx^2} + \frac{2P}{9Eb(\frac{1}{2}d - v)^2} = 0 \tag{4}$$

while that of the uncracked part of the column may be written as

$$\frac{d^2v}{dx^2} + \frac{Pv}{EI} = 0. \tag{5}$$

Integration of equation (4) results in

$$\left(\frac{dv}{dx}\right)^2 = 2A\left(\frac{1}{\frac{1}{2}d - \delta} - \frac{1}{\frac{1}{2}d - v}\right) \tag{6}$$

where $A = 2P/9Eb = \text{const.}$, and the integration constant of the previous operation satisfies $(dv/dx)_{x=0} = 0$.

Quadrature of equation (5) leads to

$$\left(\frac{dv}{dx}\right)^2 = -\frac{P}{EI}v^2 + C_1. \tag{7}$$

The slopes from equations (6) and (7) are identical at the section where the cracked and uncracked zones meet, that is, at $v = d\beta/6$ where $\beta = 1 + \sigma_t/\sigma_{av}$. By equating the equations (6)

and (7) and setting $v = d\beta/6$, C_1 can be found and the slope for the uncracked portion will now be

$$\frac{dv}{dx} = -\sqrt{\frac{3A}{2d}}\sqrt{\frac{4d/3}{\frac{1}{2}d-\delta}+\beta^2-\frac{4}{\beta_1}-v^2\frac{36}{d^2}} \tag{8}$$

where $\beta_1 = (3-\beta)/2$.

On separating the variables in equation (8), integrating, and satisfying $x|_{v=e} = L$, we get for the uncracked part,

$$x\sqrt{\frac{54A}{d^3}} = L\sqrt{\frac{54A}{d^3}} + \sin^{-1}\frac{e}{\frac{d}{6}\sqrt{\frac{\delta(4/\beta_1-\beta^2)-d(2/\beta_1-4/3-\frac{1}{2}\beta^2)}{\frac{1}{2}d-\delta}}}$$

$$-\sin^{-1}\frac{v}{\frac{d}{6}\sqrt{\frac{\delta(4/\beta_1-\beta^2)-d(2/\beta_1-4/3-\frac{1}{2}\beta^2)}{\frac{1}{2}d-v}}}. \tag{9}$$

In equation (6) the variables can also be separated. Thus, for the cracked part, integration results in

$$x = \frac{1}{\sqrt{2A}}\left[\frac{1}{t^2}\sqrt{z}\sqrt{(t^2z-1)}+\frac{1}{t^3}\ln\left(t\sqrt{z}+\sqrt{(t^2z-1)}\right)\right]+C_2$$

$$= \frac{1}{\sqrt{2A}}H(z)+C_2 \tag{10a}$$

where $t^2 = (\frac{1}{2}d-\delta)^{-1}$, $z = \frac{1}{2}d - v$, and C_2 = integration constant. The latter can be found by realizing, as before, that at $v = d\beta/6$ the cracked and uncracked zones meet, and therefore equations (9) and (10a) must result in an identical x. This leads to

$$C_2 = L\sqrt{\frac{d^3}{54A}}\left(\sin^{-1}\frac{e}{\frac{d}{6}\sqrt{\frac{\delta(4/\beta_1-\beta^2)-d(2/\beta_1-4/3-\frac{1}{2}\beta^2)}{\frac{1}{2}d-\delta}}}\right.$$

$$\left.-\sin^{-1}\frac{\beta}{\sqrt{\frac{\delta(4/\beta_1-\beta^2)-d(2/\beta_1-4/3-\frac{1}{2}\beta^2)}{\frac{1}{2}d-\delta}}}\right)-\frac{1}{\sqrt{2A}}H(d\beta_1/3). \tag{10b}$$

The load–deflection relationship can be obtained from the fact that in the cracked region $(v)_{x=0} = \delta$. On substituting these values of x and v in equation (10a) we obtain

$$L\sqrt{\frac{P}{EI}} = \sin^{-1}\left[\beta\left(\frac{\frac{\delta}{d}\left(\frac{4}{\beta_1}-\beta^2\right)-\left(\frac{2}{\beta_1}-\frac{4}{3}-\frac{1}{2}\beta^2\right)}{\gamma}\right)^{-1/2}\right]$$

$$-\sin^{-1}\left[\frac{6e}{d}\left(\frac{\frac{\delta}{d}\left(\frac{4}{\beta_1}-\beta^2\right)-\left(\frac{2}{\beta_1}-\frac{4}{3}-\frac{\beta^2}{2}\right)}{\gamma}\right)^{-1/2}\right]+3\sqrt{\gamma\beta_1}\sqrt{\beta_1/3-\gamma}+3\sqrt{3\gamma^3}\ln\frac{\sqrt{\beta_1/3}+\sqrt{\beta_1/3-\gamma}}{\sqrt{\gamma}}$$

where $\gamma = \frac{1}{2}-\frac{\delta}{d}$. (11)

If the material can resist tension neither inside the column nor on the convex face, $\sigma_t = 0$, and equation (11) reduces to

$$L\sqrt{\frac{P}{EI}} = \sin^{-1}(4/3\gamma - 3)^{-1/2} - \sin^{-1}\left[\frac{6e}{d}(4/3\gamma - 3)^{-1/2}\right] + 3\sqrt{\gamma\nu} + 3\sqrt{3\gamma^3}\ln\frac{\sqrt{\frac{1}{3}} + \sqrt{\nu}}{\sqrt{\gamma}} \tag{12}$$

where $\nu = \frac{\delta}{d} - \frac{1}{6}$.

Based on equation (12) the load v. δ/d relationship has been plotted in Fig. 2 for certain fixed values of e/d. Only the stable equilibrium paths are shown.

If, finally, the load has no eccentricity, and $\sigma_t = 0$. the second term on the RHS of equation (12) will vanish.

It should be noted that because of the presence of σ_{av} in the RHS of equation (11) the load P occurs on both sides, that is,

$$L\sqrt{\frac{P}{EI}} = f\left(\frac{e}{d}, \frac{\delta}{d}, \frac{P}{bd}, \sigma_t\right). \tag{13}$$

A small rearrangement will change it to

$$\lambda\sigma_{av} = \frac{\sigma_t}{12}f^2\left(\frac{e}{d}, \frac{\delta}{d}, \sigma_{av}, \sigma_t\right) \tag{13a}$$

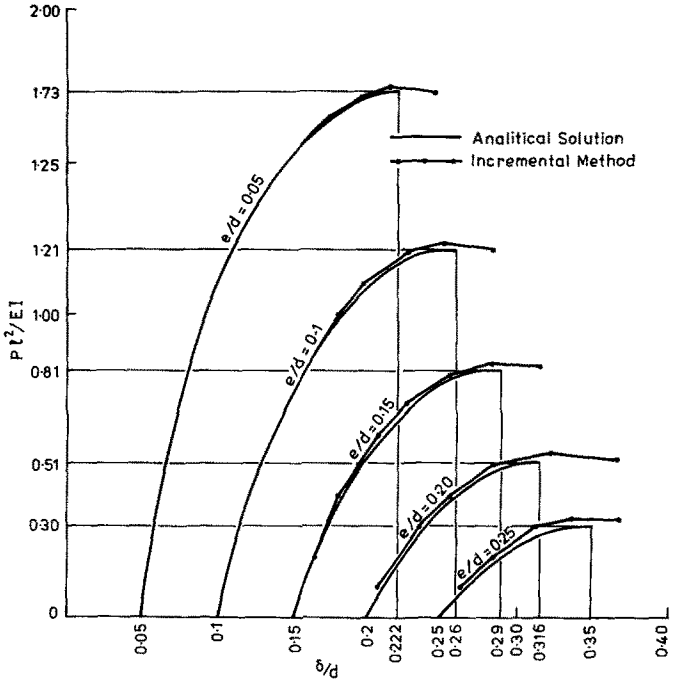

Fig. 2. Load vs deflection for various eccentricity ratios.

where $\lambda = L^2\sigma_t/d^2E$. For particular values of λ, e/d, and σ_t a relationship between σ_{av} and δ/d can be obtained.

The upper limit of stable equilibrium (Fig. 2) is reached at

$$P_{max} = 19\frac{EI}{L^2}(0{\cdot}5 - e/d)^3 \qquad (0{\cdot}01 < e/d < 0{\cdot}3). \tag{14a}$$

The following δ/d and σ belong to this limiting force:

$$(\delta/d)_{max} = 0{\cdot}194 + 0{\cdot}612\frac{e}{d} \qquad (0{\cdot}01 < e/d < 0{\cdot}3) \tag{14b}$$

and

$$\sigma_{max} = \frac{1{\cdot}72E}{(L/d)^2}(0{\cdot}5 - e/d)^2 \qquad (0{\cdot}01 < e/d < 0{\cdot}3). \tag{14c}$$

Equation (14b) may be compared with $0{\cdot}188 + 0{\cdot}625\frac{e}{d}$ of Ref. [3]. Equations (14) apply for $\sigma_t = 0$.

3. MATRIX FORMULATION

If a uniform bar of length l is oriented in the x direction and an initial F acts in the x direction (Fig. 3), the strain energy due to small bending becomes

$$U = \frac{1}{2}EI\int_0^l \left(\frac{d^2y}{dx^2}\right)^2 dx + \frac{1}{2}F\int_0^l \left(\frac{dy}{dx}\right)^2 dx.$$

The exact shape for simple flexure is

$$y = u_3 + \theta_1 x - \frac{x^2}{l}\left[2\theta_1 + \theta_2 + \frac{3u_3}{l} - \frac{3u_4}{l}\right] + \frac{x^3}{l^2}\left[\theta_1 + \theta_2 + \frac{2u_3}{l} - \frac{2u_4}{l}\right]. \tag{10}$$

From $S_j = \partial U/\partial u_j$ the force–displacement relationship can be had in the form

$$\mathbf{P} = [k_E + k_G]\mathbf{u} \tag{15}$$

where $\mathbf{P} = \{m_1, m_2, p_3, p_4\}$ $\mathbf{u} = \{\theta_1, \theta_2, u_3, u_4\}$; k_E and k_G are the elastic and geometric stiffness matrices, respectively.

To assess the effectiveness of this method consider the simple column fixed at the bottom and subject to an eccentric load P (Fig. 4a, b). For an element whose joint displacements are identified by 1, 2, 3 and 4, and which is subject to an axial force F (Fig. 3), the elastic and

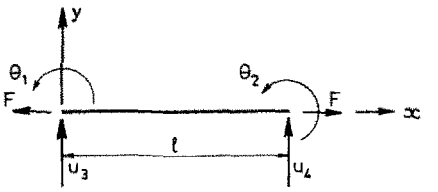

Fig. 3. Assumed degrees of freedom of a column element.

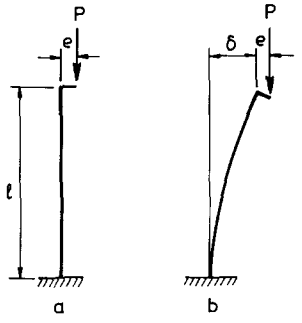

Fig. 4. Eccentric load applied to column.

geometric member stiffnesses are as follows:

$$k_E = \frac{EI}{l}\begin{bmatrix} 4 & & \text{symm.} & \\ 2 & 4 & & \\ 6/l & 6/l & 12/l^2 & \\ -6/l & -6/l & -12/l^2 & 12/l^2 \end{bmatrix} \qquad k_G = \frac{F}{10l}\begin{bmatrix} 4l^2/3 & & \text{symm.} & \\ -l^2/3 & 4l^2/3 & & \\ l & l & 12 & \\ -l & -l & -12 & 12 \end{bmatrix}$$

where positive F represents a tensile force.

From equation (15), by inversion, we find

$$\begin{bmatrix} \theta_2 \\ u_4 \end{bmatrix} = [k_E + k_G]^{-1}\begin{bmatrix} -M_0 \\ 0 \end{bmatrix} = \begin{bmatrix} a_{11} & a_{12} \\ a_{21} & a_{22} \end{bmatrix}\begin{bmatrix} -M_0 \\ 0 \end{bmatrix}. \tag{16}$$

With $m_2 = -M_0 = -eF$, and $\mu = Fl^2/EI$

$$a_{21} = \frac{l}{EI}\frac{l(6-0{\cdot}1\mu)}{12-\frac{26}{5}\mu+\frac{3}{20}\mu^2} \quad \text{and} \quad u_4 = -e\mu\frac{(6-0{\cdot}1\mu)}{12-\frac{26}{5}\mu+\frac{3}{20}\mu^2}.$$

Comparing now u_4 with the analytical result of $\delta = e(\sec\sqrt{(Pl/EI)}-1)$ we find

$$\sec\sqrt{\mu}-1 = \frac{1}{2}\mu+\frac{5}{24}\mu^2+\frac{61}{120}\mu^3+\frac{277}{8064}\mu^4+\cdots$$

while

$$-\frac{u_4}{e} = \frac{1}{2}\mu+\frac{5}{24}\mu^2+\frac{60{\cdot}5}{720}\mu^3+\frac{272{\cdot}62}{8064}\mu^4+\cdots$$

These two series look almost identical, nevertheless they may deviate because $\mu_{max} \approx 2{\cdot}46$. If $\mu = 2{\cdot}4$ and the first series is replaced by $\sec\sqrt{\mu}$ direct substitution in the expression of a_{21} will result in an error of 22 per cent.

If the column is idealized into two elements and carries a load F with eccentricity $-e$, the

deflection u_4 (Fig. 5), after establishing the global stiffness K_E and K_G is found to be

$$u_4 = -e\mu \frac{288 - 57{\cdot}6\mu + 3{\cdot}28\mu^2 - 0{\cdot}04\mu^3}{144 - 268{\cdot}8\mu + 59{\cdot}2\mu^2 - 3{\cdot}2\mu^3 + 0{\cdot}0425\mu^4}. \tag{17}$$

Since

$$L = 2l, \sec\sqrt{4\mu} - 1 = 2\mu + \frac{10}{3}\mu^2 + 5{\cdot}4222\mu^3 + 8{\cdot}7936\mu^4 + \cdots$$

while

$$-\frac{u_4}{e} = 2\mu + \frac{10}{3}\mu^2 + 5{\cdot}42278\mu^3 + 8{\cdot}7963\mu^4 + \cdots$$

Bearing in mind that for a two-element column $\mu_{max} = \pi^2/16 = 0{\cdot}615$, the two series are practically identical.

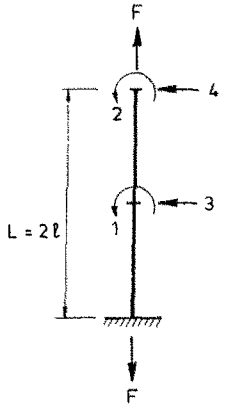

Fig. 5. The two-element column showing degrees of freedom.

4. INCREMENTAL PROCEDURE

The exact analysis is, as seen, complicated, even though idealized loading and boundary conditions have been applied. A modified stiffness method will be developed here which, if successful, may be adapted for more complex loading and boundary conditions. The procedure will be applied to a four-element idealized column made of a material of little or no tensile strength (Fig. 6). The moments of inertia of the members are uniform over the element but not, as a rule, identical because the active cross section varies. The horizontal elements, s, are rigid connectors; they vary in length and represent the shift in the axes of the active cross sections. The structural (global) stiffness is given in Table 1.

The basic equation in the incremental method is

$$\Delta\mathbf{F}_i = [K_{E,i-1} + K_{G,i-1}]\Delta\mathbf{u}_i \tag{18}$$

where i is the step number. In the incremental procedure the load–deformation relation of the ith step is based on the stiffness of the $(i-1)$th step. By gradually increasing F, that is μ, the deflections may be calculated from equation (18). After the ith step the deflected shape is shown

Table 1

$$\frac{EI}{l}\begin{bmatrix}
4(\alpha_1+\alpha_2)-\frac{4}{15}\mu & & & & & & & \\
2\alpha_1+\frac{\mu}{30} & 4\alpha_1-\frac{2}{15}\mu & & & & \text{symmetrical} & & \\
\frac{1}{l}[6(\alpha_1-\alpha_2)] & \frac{1}{l}\left(6\alpha_1-\frac{\mu}{10}\right) & \frac{1}{l^2}[12(\alpha_1+\alpha_2)-2{\cdot}4\mu] & & & & & \\
\frac{1}{l}\left[-6\alpha_1+\frac{\mu}{10}\right] & \frac{1}{l}\left(-6\alpha_1+\frac{\mu}{10}\right) & \frac{1}{l^2}(-12\alpha_1+1{\cdot}2\mu) & \frac{1}{l^2}(12\alpha_1-1{\cdot}2\mu) & & & & \\
2\alpha_2+\frac{\mu}{30} & 0 & \frac{1}{l}\left(-6\alpha_2+\frac{\mu}{10}\right) & 0 & 4(\alpha_2+\alpha_3)-\frac{4}{15}\mu & & & \\
\frac{1}{l}\left(6\alpha_2-\frac{\mu}{10}\right) & 0 & \frac{1}{l^2}(-12\alpha_2+1{\cdot}2\mu) & 0 & \frac{1}{l}[6(\alpha_2-\alpha_3)] & \frac{1}{l^2}[12(\alpha_2+\alpha_3)-2{\cdot}4\mu] & & \\
0 & 0 & 0 & 0 & 2\alpha_3+\frac{\mu}{30} & \frac{1}{l}\left(-6\alpha_3+\frac{\mu}{10}\right) & 4(\alpha_3+\alpha_4)-\frac{4}{15}\mu & \\
0 & 0 & 0 & 0 & \frac{1}{l}\left(6\alpha_3-\frac{\mu}{10}\right) & \frac{1}{l^2}(-12\alpha_3+1{\cdot}2\mu) & \frac{1}{l}[6(\alpha_3-\alpha_4)] & \frac{1}{l^2}\begin{bmatrix}12(\alpha_3+\alpha_4)\\-2{\cdot}4\mu\end{bmatrix}
\end{bmatrix}$$

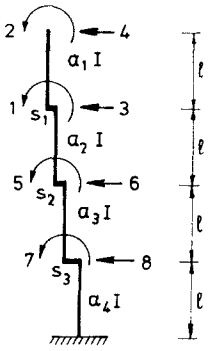

Fig. 6. The four-element column with rigid connectors.

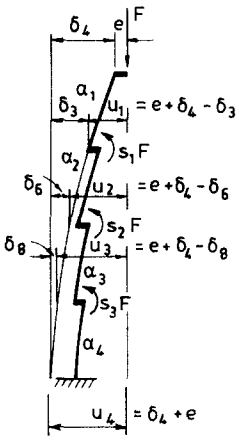

Fig. 7. Deflection of the four-element column.

in Fig. 7. At joint displacements 1, 5 and 7 couples s_1F, s_2F, and s_3F, respectively, have been applied to take care of the shift in the axes. Figure 8 shows the changing values of $d_{m,i}$, $\alpha_{m,i}$, and $s_{m,i}$, where $m = 1, 2, 3, 4$ (member), and i is the step number. The transitions of the effective depths in Fig. 8 are based on a material that can resist zero tension only. For this case

$$\alpha_{m,i} = \left(\frac{d_{m,i}}{d}\right)^3 \leqslant 1$$

$$s_{m,i} = \tfrac{1}{2}(d_{m,i} - d_{m+1,i}) \geqslant 0 \tag{19}$$

$$d_{m,i} = 1{\cdot}5 d_{m,i-1} - 3u_{m,i-1} \leqslant d_{m-1,i}.$$

If the material can resist tension, $\sigma_t > 0$, then

$$d_{m,i} = d \quad \text{and} \quad \alpha_{m,i} = 1 \quad \text{if} \quad u_{m,i-1} \leqslant \frac{d}{6}\left(1 + \sigma_t \frac{bd}{F}\right)$$

$$d_{m,i} = 1{\cdot}5 d_{m,i-1} - 3u_{m,i-1} \quad \text{if} \quad u_{m,i-1} > \frac{d}{6}\left(1 + \sigma_t \frac{bd}{F}\right). \tag{20}$$

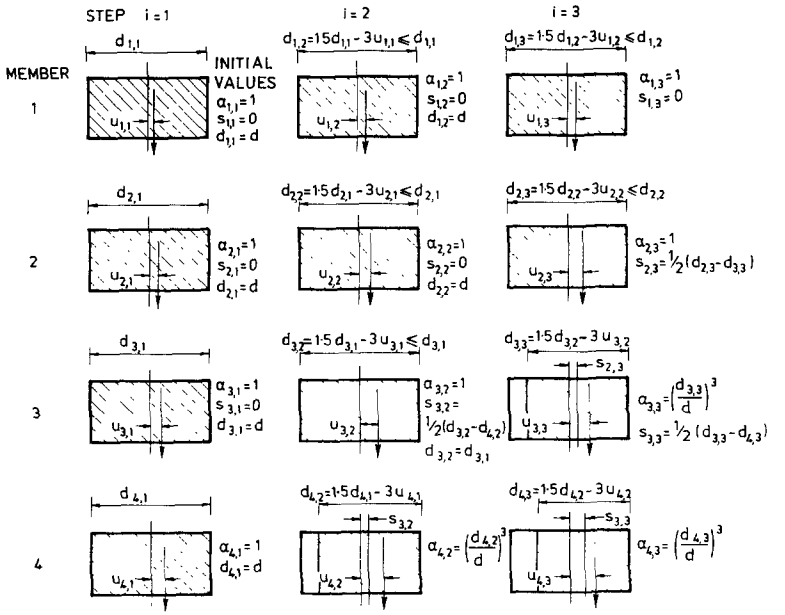

Fig. 8. Cross section geometry during incremental steps 1, 2 and 3.

That means that $\alpha < 1$ will enter the iterative process at a later stage.

No coordinate transformation is needed between steps because deformations are "small".

The formulation and procedure developed above has been applied to the case of an eccentrically loaded column of no-tension material. The same problem has previously been solved by analytical methods so that a comparison was possible. Both results are plotted in Fig. 2.

It is known that the tangent modulus at failure is about 70 per cent of the initial value[11], hence the stress–strain curve for bricks is not linear. The incremental approach allows certain refinements not available in the analytical solution; as the average stress increase, step by step, E can be modified accordingly.

5. CONCLUSION

The complexity of non-linear differential equations yield analytical solutions in a few special cases only. The present method will, with suitable modifications, cater for more complicated problems in the field of masonry structures, such as the inclusion of lateral loads and the dead weight of the structure.

The greater strength of the brick units as against the mortar beds connecting them results in a discontinuity in strength and stiffness. The resulting stress distribution has been replaced by an idealized distribution.

REFERENCES

1. K. Angervo, *Ueber die Knickung und Tragfahigkeit eines excentrisch gedrueckten Pfeilers.* Staatliche Technische Forschungsanstalt, Helsinki (1954).
2. J. C. Chapman and J. Slatford, The elastic buckling of brittle columns, *Proc. Inst. Civ. Eng.* **6**, 107 (1957).
3. F. Y. Yokel, Stability and load capacity of members with no tensile strength, *Proc. A.S.C.E.* **97,ST7**, 1913 (1971).
4. S. Risager, The buckling load of linear elastic walls without tensile strength. *Proc. 2nd Int. Brick and Masonry Conf.* p. 133. The British Ceramic Research Assoc. Stoke-on-Trent (1971).

5. Bo-Goeran Hellers, Eccentrically compressed columns without tensile strength subjected to uniformly distributed lateral loads. *National Swedish institute for Building Research*, 35 (1967).
6. S. Sahlin, Transversely loaded compression members made of materials having no tensile strength, *IABSE* **21**, 243 (1961).
7. S. Sahlin and B. G. Hellers, Buckling of a two-hinged frame with verticals having no tensile strength. *Inst. Struc. Build.* No. 60. Stockholm (1966).
8. R. H. Gallagher and J. Padlog, Discrete element approach to structural instability analysis, *AIAA J.* **1**, 1437 (1963).
9. T. Y. Yang, Matrix displacement solution to elastica problems, *Int. J. Solids Struct.* **9**, 829 (1973).
10. F. W. Beaufait, W. H. Rowan, P. G. Hoadley and R. M. Hackett, *Computer Methods of Structural Analysis*, p. 394. Prentice-Hall (1970).
11. F. Y. Yokel, R. G. Mathey and R. D. Dikkers, Strength of masonry walls under compressive and transverse loads. *Building Science Series* 34. Nat. Bureau of Standards (1971).